Eur. Phys. J. Special Topics **227**, 353–363 (2018)

https://doi.org/10.1140/epjst/e2018-00094-2

THE EUROPEAN PHYSICAL JOURNAL SPECIAL TOPICS

Regular Article

Exact spin-orbit qubit manipulation

Anton Ramšak[1,2,a], Tilen Čadež[3], Ambrož Kregar[4,5], and Lara Ulčakar[2]

[1] Faculty of Mathematics and Physics, University of Ljubljana, Ljubljana, Slovenia
[2] Jožef Stefan Institute, Ljubljana, Slovenia
[3] Beijing Computational Science Research Center, Beijing 100193, P.R. China
[4] Faculty of Education, University of Ljubljana, Ljubljana, Slovenia
[5] Faculty of Mechanical Engineering, University of Ljubljana, Ljubljana, Slovenia

Received 16 October 2017 / Received in final form 10 January 2018
Published online 28 September 2018

Abstract. We consider exactly solvable manipulation of spin-qubits confined in a moving harmonic trap and in the presence of the time dependent Rashba interaction. Non-adiabatic Anandan phase for cyclic time evolution is compared to the Wilczek-Zee adiabatic counterpart. It is shown that the ratio of these two phases can for a chosen system be any real number. Next we demonstrate the possibility of arbitrary qubit transformation in a ring with spin-orbit interaction. Finally, we present an example of exact analysis of spin-orbit dynamics influenced by the Ornstein-Uhlenbeck coloured noise.

1 Introduction

Spintronics as a promissing new branch of electronics has the potential for realising building blocks of a quantum computer via electron spin qubits. Implementation of such qubits is feasible in gated semiconductor devices based on quantum dots and quantum wires [1,2]. Qubit manipulation may be achieved through rotation of the electron's spin by the application of an external magnetic field [3] or by methods where magnetic field is replaced by the usage of the spin-orbit interaction (SOI) [4,5]. In spintronic devices the SOI is particularly suitable for qubit manipulation since it can be tuned locally via electrostatic gates [6–15]. Systems with such electron manipulation have been already experimentally realized in various semiconducting devices [16–20].

Recently a scheme was proposed, where non-adiabatic qubit manipulation is achieved by translating a qubit in one dimension [21,22] in the presence of time dependent Rashba interaction [23,24]. For quantum dots with harmonic confining potential the exact analytical solution enables also the analysis of the non-adiabatic non-Abelian Anandan phase [25]. The qubit transformations in such linear systems are limited to the cases of spin rotations around a fixed axis and most recently this limitation posed by fixed axis was eliminated in transformations on a quantum ring structure [26,27].

In view of the fact that exact solutions for qubit manipulation are known, also the analysis of certain environment effects can be considered analytically [28]. Errors

[a] e-mail: anton.ramsak@fmf.uni-lj.si

in the qubit manipulation can be caused by fluctuating electric fields, created by the piezoelectric phonons [9,29–31] or due to phonon-mediated instabilities in molecular systems with phonon assisted potential barriers, which introduce noise in the confining potentials [32,33]. Electrons could be also carried by the surface acoustic waves, where the noise can arise due to time dependence in the electron-electron interaction effects [34–36].

In this paper we concentrate on some explicit types of qubit transformation drivings, in one dimension and in a ring system. In particular, after the introduction we present the model in Section 2, show exact solutions of the time dependent Schrödinger equation and analyse the Anandan phase. In Section 3 we demonstrate the feasibility of arbitrary qubit transformation in a ring system. Finally, in Section 4 it is shown how the errors due to coloured noise in drivings can be analysed exactly. Section 5 is devoted to the summary.

2 Anandan phase in a linear system

We concentrate on qubits represented as spin states of an electron in a harmonic trap [21,22]. The position of the trap $\xi(t)$ in the one-dimensional quantum wire is time dependent and is controlled by the application of external electric fields. The spin is controlled by the spin-orbit interaction related to the external electric field. Hamiltonian of the system is

$$H(t) = \frac{p^2}{2m^*} I + \frac{m^*\omega^2}{2}[x - \xi(t)]^2 I + \alpha(t) p\, \mathbf{n}\cdot\boldsymbol{\sigma}, \tag{1}$$

where m^* is the electron effective mass, ω is the frequency of the harmonic trap and $\alpha(t)$ is the strength of the time dependent Rashba spin-orbit interaction. $\boldsymbol{\sigma}$ and I are Pauli spin matrices and unity operator in spin space, respectively. The spin rotation axis $\mathbf{n}$ is constant and depends on the crystal structure of the quasi-one-dimensional material used and the direction of the applied electric field [16]. Exact solution corresponding to the Hamiltonian in equation (1) is given by [21,22],

$$|\Psi_{ms}(t)\rangle = e^{-i\omega_m t}\mathcal{A}_\alpha(t)\mathcal{X}_\xi(t)|\psi_m(x)\rangle|\chi_s\rangle, \tag{2}$$

where

$$\mathcal{A}_\alpha(t) = e^{-i[(\phi_\alpha(t)+m^*\dot{a}_c(t)a_c(t)/\omega^2)I+\phi(t)\mathbf{n}\cdot\boldsymbol{\sigma}/2]} e^{-i\dot{a}_c(t)p\mathbf{n}\cdot\boldsymbol{\sigma}/\omega^2} e^{-im^* a_c(t)x\mathbf{n}\cdot\boldsymbol{\sigma}}, \tag{3}$$

$$\mathcal{X}_\xi(t) = e^{-i\phi_\xi(t)} e^{im^*[x-x_c(t)]\dot{x}_c(t)} e^{-ix_c(t)p} I. \tag{4}$$

Here $\psi_m(x)$ represents the m-th eigenstate of a harmonic oscillator with energy $\omega_m = (m+1/2)\omega$ and $|\chi_s\rangle$ is a spinor of the electron in the eigenbasis of operator σ_z. The solution is determined by two unitary transformations, of spin part $\mathcal{A}_\alpha$ and charge contribution $\mathcal{X}_\xi$ which translate the system into the "moving frame" of both SOI and position and transform the Hamiltonian equation (1) into a simple time independent harmonic oscillator Hamiltonian. The phase $\phi_\xi(t) = -\int_0^t L_\xi(t')\mathrm{d}t'$ is the coordinate action integral, with $L_\xi(t) = m^*\dot{x}_c^2(t)/2 - m^*\omega^2[x_c(t)-\xi(t)]^2/2$ being the Lagrange function of a driven harmonic oscillator and $x_c(t)$ is the solution to the equation of motion of a classical driven oscillator

$$\ddot{x}_c(t) + \omega^2 x_c(t) = \omega^2\xi(t). \tag{5}$$

Another phase factor is the SOI action integral phase $\phi_\alpha(t) = -\int_0^t L_\alpha(t')\mathrm{d}t'$, where $L_\alpha(t) = m^*\dot{a}_c^2(t)/(2\omega^2) - m^*[a_c(t)-\alpha(t)]^2/2 + m^*\alpha^2(t)/2$ is the Lagrange function

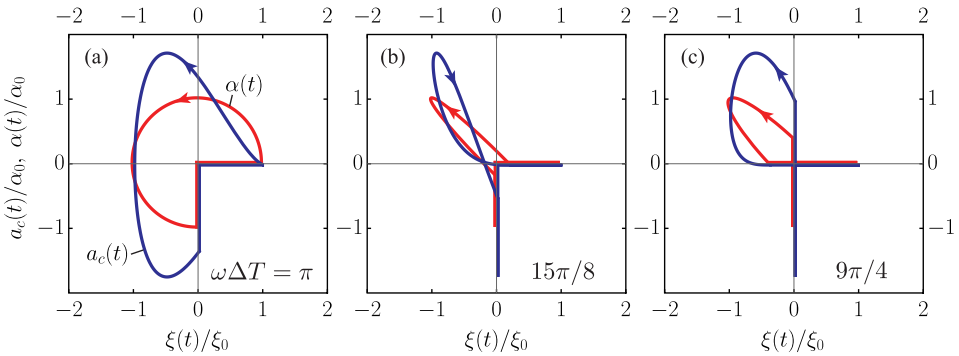

Fig. 1. Contours $[\xi(t)/\xi_0, \alpha(t)/\alpha_0]$ and $[\xi(t)/\xi_0, a_c(t)/\alpha_0]$. Panels (a), (b), (c) correspond to different values of $\omega\Delta T = \pi, 15\pi/8, 9\pi/4$, respectively. Note the reversed direction of motion $a_c[\xi]$ in (b) resulting in the negative Anandan phase.

of another driven oscillator, satisfying

$$\ddot{a}_c(t) + \omega^2 a_c(t) = \omega^2 \alpha(t). \tag{6}$$

Spin-qubits are rotated around $\mathbf{n}$ by terms proportional to operators $a_c(t)x$, $\dot{a}_c(t)p$ and the phase $\phi(t)$. Here we consider only cyclic drivings and cyclic resposes, characterised by conditions $\xi(t+T) = \xi(t)$, $\alpha(t+T) = \alpha(t)$, $x_c(t+T) = x_c(t)$, $a_c(t+T) = a_c(t)$ and $\dot{x}_c(t+T) = \dot{x}_c(t)$, $\dot{a}_c(t+T) = \dot{a}_c(t)$. The angle of spin rotation is then given by the Anandan phase [22,25],

$$\phi = \phi(T) = -2m^* \int_0^T \dot{a}_c(t)\xi(t)\mathrm{d}t = 2m^* \oint_{\mathcal{C}} a_c[\xi]\mathrm{d}\xi, \tag{7}$$

where $a_c[\xi]$ represents the contour $\mathcal{C}$ in 2D parametric space $[\xi(t), a_c(t)]$ for $0 \le t \le T$. Thus the spin rotation angle is determined by the area enclosed by $\mathcal{C}$. In the limit of a very slow motion this contour will reduce to the driving curve $\alpha[\xi]$ and in this limit the area enclosed by the contour represents the Wilczek-Zee non-Abelian phase [37], *i.e.*, the adiabatic result $\phi(T) \to \phi_{\rm ad}$ in the limit $T \to \infty$.

A challenging question here is: "Which – the Anandan phase ϕ or the adiabatic $\phi_{\rm ad}$ phase – is for a particular driving curve larger?" A simple general rule for a given driving does not seem to be available without explicitly comparing the solutions. However, in order to elucidate this question to some extent generally we consider a family of contours of broken circular shapes represented by driving parametrized as

$$\begin{aligned} \xi(t) &= \xi_0 \sin(\omega t/2)\, \Theta(t)\Theta(2T_1 - t), \\ \alpha(t) &= \alpha_0 \xi(t - \Delta T)/\xi_0, \end{aligned} \tag{8}$$

where $\Theta(t)$ is the Heaviside step function, $T_1 = 2\pi/\omega$ and ΔT is the time delay. The driving is applied periodically with the cycle period $T = 2T_1 + \Delta T$. The responses are periodic and within one cycle given by

$$\begin{aligned} x_c(t) &= \frac{2}{3}\xi_0 \left[2\sin(\omega t/2) - \sin(\omega t)\right] \Theta(t)\Theta(2T_1 - t), \\ a_c(t) &= \alpha_0 x_c(t - \Delta T)/\xi_0. \end{aligned}$$

Various contours $[\xi(t)/\xi_0, a_c(t)/\alpha_0] \sim \mathcal{C}$ and $[\xi(t)/\xi_0, \alpha(t)/\alpha_0] \sim \mathcal{C}_{\rm ad}$ are for different ΔT presented in Figure 1. In the panel Figure 1b note the reversion of the direction

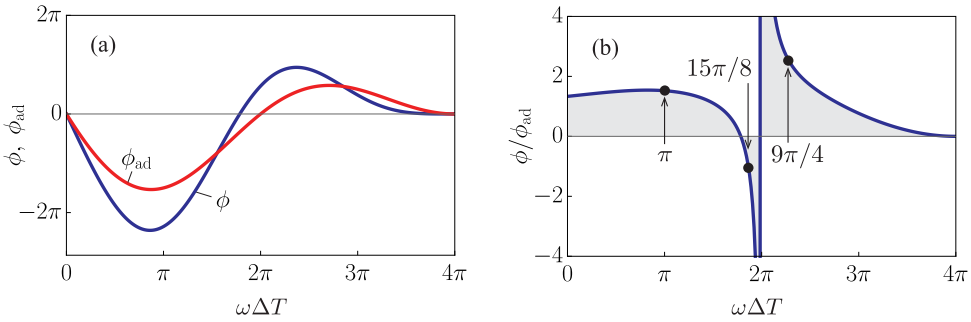

Fig. 2. In panel (a) the Anandan phase ϕ and the Wilczek-Zee (adiabatic) phase $\phi_{\rm ad}$ are plotted as a function of the delay $\omega\Delta T$. The phases are scaled by the factor $m^*\xi_0\alpha_0$. Note two points of equality where $\phi = \phi_{\rm ad}$ and that the phases change sign at different ΔT. In panel (b) the ratio $\phi/\phi_{\rm ad}$ is presented. Note the pole at $\omega\Delta T = 2\pi$, where $\phi_{\rm ad} = 0$. Arrows indicate values of $\omega\Delta T$ corresponding to special cases shown in Figure 1.

of motion along contour $\mathcal{C}$ with respect to $\mathcal{C}_{\rm ad}$ which results in *negative* Anandan phase. In all panels the beginning and the end of a cycle is at $\xi/\xi_0 = 1$ and $\alpha = 0$ with $x_c(0) = \dot{x}_c(0) = 0$ and $a_c(0) = \dot{a}_c(0) = 0$.

The quantum phases ϕ and $\phi_{\rm ad}$, calculated as a function of the delay $\omega\Delta T$, are presented in Figure 2a. There are two important points to be noted: (i) Both curves are similar in the sense that particular phase for small ΔT is negative and by progressively larger time delay at some point changes sign and finally vanishes at $\Delta T = 2T_1$, where there is no overlap between $\xi(t)$ and $a_c(t)$. (ii) The phase curves intersect, which proves that ϕ and $\phi_{\rm ad}$ can be equal for some type of driving and, moreover, the ratio $\phi/\phi_{\rm ad}$, shown in Figure 2b, can take *any value, positive* or *negative*. Since the amplitudes of drivings, ξ_0 and α_0, are additional free parameters, one can by changing ΔT tune the phases independently of each other to any value.

3 Arbitrary qubit transformations

Spin transformations of an electron, driven along a straight wire, are limited to rotations around a fixed axis $\mathbf{n}$, meaning that electron's spin cannot be rotated for an arbitrary angle. One way to lift this restriction is to move the electron in two spatial dimensions. Here we consider ring systems as one of the simplest choices.

Cylindrical coordinates r and φ are a natural parametrisation to describe the electron moving along a ring. The restriction of electron's motion to the ring is achieved by strong binding potential in the radial direction, resulting in the electron occupying the lowest radial eigenstate. Angular part of the wavefunction is then governed by an effective Hamiltonian [38]

$$H = \frac{p_\varphi^2}{2m^*} I + \alpha(t)\left(\sigma_\rho p_\varphi - \frac{i}{2}\frac{1}{R}\sigma_\varphi\right) + V(\varphi, t) I. \tag{9}$$

This Hamiltonian is effectively one-dimensional, describing the motion of the electron along the periodic coordinate φ with its conjugate momentum $p_\varphi = -i\frac{1}{R}\frac{\partial}{\partial\varphi}$. The spin operators in the cylindrical coordinate system are given by

$$\sigma_\rho(\varphi) = \quad \sigma_x \cos\varphi + \sigma_y \sin\varphi, \tag{10}$$
$$\sigma_\varphi(\varphi) = -\sigma_x \sin\varphi + \sigma_y \cos\varphi. \tag{11}$$

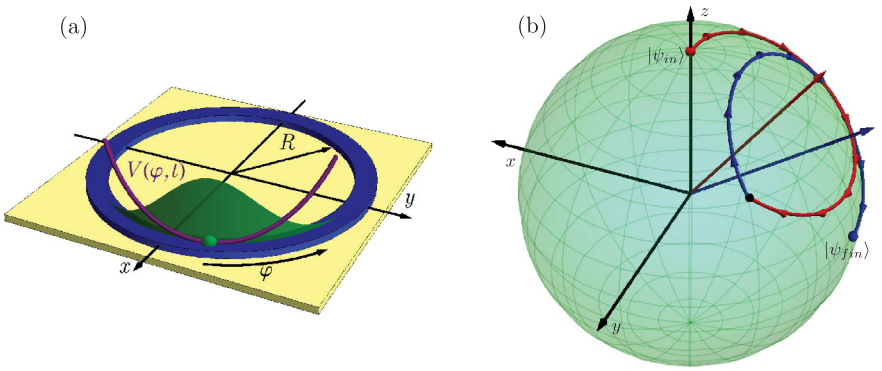

Fig. 3. (a) Schematic presentation of the system. The position of the electron (green point), confined by potential well V (purple) on a ring of radius R, is described by coordinate φ. (b) One representation of the qubit Hadamard transformation on the Bloch sphere, using the Rashba-dependent rotations $U_i^\dagger$. First the electron at some α_1 is shifted by an angle $\Delta\varphi_1$, causing a rotation around the axis $\mathbf{n_1}$ (red path). The Rashba coupling is then adiabatically changed to α_2 and the electron is shifted by $\Delta\varphi_2$ causing additional rotation around $\mathbf{n_2}$ (blue path).

Time dependent potential $V(\varphi, t)$ is a small perturbation to the confining potential, restricting the electron to the ring, and is used to manipulate the electron's position on the ring. Like in Section 2, the motion of the electron is driven by an electric field locally expressed as the harmonic potential with time dependent position as is schematically shown in Figure 3a, with

$$V(\varphi, t) = \frac{m^*\omega^2}{2}\left[\varphi - \xi(t)\right]^2. \tag{12}$$

In order to solve the Schrödinger equation, we first transform the Hamiltonian with a time independent transformation

$$\mathcal{Z}_\varphi = \exp\left(-i\frac{\varphi}{2}\sigma_z\right), \tag{13}$$

which maps the spin operators from cylindrical to Cartesian coordinates. This results in a Hamiltonian, very similar to equation (1),

$$H'(t) = \mathcal{Z}_\varphi^\dagger H(t)\mathcal{Z}_\varphi = \frac{p_\varphi^2}{2m^*}I + \frac{m^*R^2\omega^2}{2}[\varphi - \xi(t)]^2 I + p\,\boldsymbol{\alpha}(t)\cdot\boldsymbol{\sigma} + \frac{1}{8m^*R^2}I. \tag{14}$$

Contrary to the Hamiltonian for a linear system, $H'(t)$ has a time-dependent rotation axis $\boldsymbol{\alpha}(t) = (\alpha(t), 0, -1)$ that can be manipulated by tuning the Rashba coupling. For such system, solutions of Schrödinger equation cannot be found using the transformations $\mathcal{A}_\alpha$ and $\mathcal{X}_\xi$. However, analytical solutions can be found for two special cases of driving $\alpha(t)$ and $\xi(t)$, the first one being for a constant Rashba coupling while the minimum of the harmonic potential is moving, and the second being an adiabatic change of the Rashba coupling in a static potential [26,27].

In order to describe the time evolution of the system, we further transform the Hamiltonian using the transformation $\mathcal{U}^\dagger(t) = \mathcal{A}_\alpha\mathcal{X}_\xi$ as in Section 2 but with a

different form of the operator

$$\mathcal{A}_\alpha = \exp\left(-i\frac{\varphi}{2}\boldsymbol{\alpha}\cdot\boldsymbol{\sigma}\right), \tag{15}$$

leading to a Hamiltonian of harmonic oscillator with a time-dependent spin-orbit energy shift

$$H''(t) = \mathcal{U}H'(t)\mathcal{U}^\dagger = \frac{p_\varphi^2}{2m^*} + \frac{m^*R^2\omega^2}{2}\varphi^2 + \frac{m^*\alpha(t)^2}{2}. \tag{16}$$

If the Rashba coupling is constant, the time-dependent wavefunction of the system can be described in a similar manner as for the linear system – a combination of eigenstates, evolving as

$$|\Psi_{ms}(t)\rangle = e^{-i\omega_m t}\mathcal{Z}_\varphi\mathcal{A}_\alpha\mathcal{X}_{\xi(t)}|\psi_m(\varphi)\rangle|\chi_s\rangle. \tag{17}$$

To describe the case of adiabatically changing Rashba coupling, it is convenient to find a basis of Kramers states, centred at some ξ_1,

$$|\tilde{\Psi}_{ms\xi_1}(t)\rangle = e^{-i\omega_m t}\mathcal{Z}_\varphi\mathcal{X}_{\xi_1}\mathcal{A}_{\alpha(t)}|\psi_m(\varphi)\rangle\mathcal{Y}_{\tilde{\vartheta}_{\alpha(t)}}|\chi_s\rangle, \tag{18}$$

for which the time evolution is manifested only as a change of the parameter $\alpha(t)$ in the operator $\mathcal{A}_{\alpha(t)}$ and in

$$\mathcal{Y}_{\tilde{\vartheta}_{\alpha(t)}} = e^{-i\tilde{\vartheta}_{\alpha(t)}\sigma_y}. \tag{19}$$

The rotation angle $\tilde{\vartheta}_{\alpha(t)}$ due to the change of the Rashba coupling can be calculated numerically and is mostly negligible in realistic systems. If the Kramers states $|\tilde{\Psi}_{ms\xi_1}(t)\rangle$ are treated as a qubit basis, the adiabatic change of the Rashba coupling only affects the basis states, but not the coefficients of the expansion c_s in the Kramers basis,

$$|\psi(\varphi,t)\rangle = e^{i\phi_\alpha(t)}\sum_s c_s|\tilde{\Psi}_{ms\xi_1}(t)\rangle. \tag{20}$$

Driving of the electron along the ring by an external potential can also be expressed in terms of the Kramers states. If the position of the electron's wavefunction before (ξ_{i-1}) and after the shift of potential minimum (ξ_i) is fixed, the transformation of the wavefunction can be written as

$$|\psi(\varphi,t)\rangle = \sum_s c_{i-1,s}|\tilde{\Psi}_{ms\xi_{i-1}}(t)\rangle \rightarrow |\psi(\varphi,t)\rangle = \sum_s c_{i,s}|\tilde{\Psi}_{ms\xi_i}(t)\rangle, \tag{21}$$

where coefficients c_s transform as $c_{i+1,s} = \sum_{s'}\chi_s^\dagger U_i^\dagger\chi_{s'}c_{i,s'}$. Writing Kramers states in the basis equation (17) shows that the operator $U_i^\dagger$ is a spin rotation for the angle γ_i around the axis $\mathbf{n}_i$ that is tilted for ϑ_{α_i} around y direction,

$$U_i^\dagger = e^{-i\frac{\gamma_i}{2}\mathbf{n}_i\cdot\boldsymbol{\sigma}}, \quad \mathbf{n}_i = (\sin\vartheta_{\alpha_i}, 0, \cos\vartheta_{\alpha_i}), \tag{22}$$

$$\vartheta_{\alpha_i} = \tilde{\vartheta}_{\alpha_i} - \arctan\left(2m^*R\alpha_i\right), \quad \gamma_i = -\Delta\varphi_i\sqrt{1+\left(2m^*R\alpha_i\right)^2}. \tag{23}$$

α_i is the value of the Rashba coupling during the shift from positions ξ_i and ξ_{i+1}.

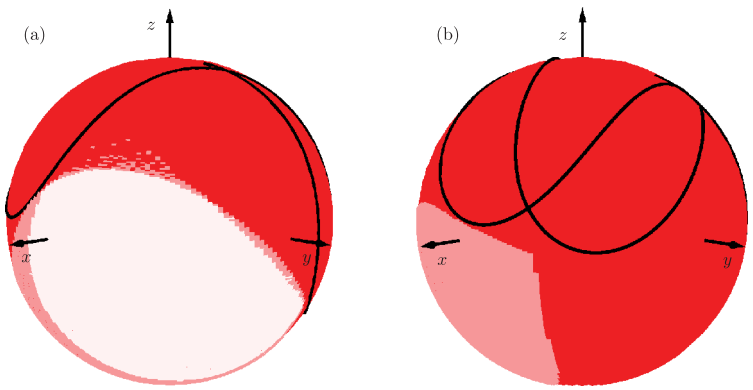

Fig. 4. Sectors of the Bloch sphere that are covered by one (a) or two (b) rotations of the electron on the ring, for factor of Rashba coupling amplification $k = 5$. Black lines represent transformations reached by $N = 2$ shifts of the electron position. Area shaded by dark red corresponds to $N = 3$ and light red to $N = 4$. For our set of N, the white area in (a) can be covered by two rotations. Numerical calculations were performed on a 200×200 grid.

If the Kramers states are considered as a qubit basis and the coefficients c_{is} parametrized as points $\mathbf{r} = (\sin\Theta\cos\Phi, \sin\Theta\sin\Phi, \cos\Theta)$ on the Bloch sphere,

$$(c_{i,\uparrow}, c_{i,\downarrow}) = \left(\cos\frac{\Theta}{2}, e^{i\Phi}\sin\frac{\Theta}{2}\right), \tag{24}$$

the rotation $U_i^\dagger$ is a simple rotation on the sphere, which gives an intuitive insight into the qubit transformations.

We performed a comprehensive numerical analysis of the transformation, which revealed that any qubit transformation can be realized using the described time evolution by properly adjusting the distances of electron shift and the accompanying values of the Rashba coupling. An example of such a transformation is shown in Figure 3b, where the Hadamard-like gate is applied to transform the qubit state $|0\rangle \rightarrow \frac{1}{\sqrt{2}}(|0\rangle - |1\rangle)$. Figure 4 shows all possible rotation angles on a Bloch sphere for a qubit, that was initially the eigenstate of spin along the z-axis. The Bloch sphere coverage was calculated using the Monte-Carlo simulation and it shows that any qubit transformation is possible to achieve. Panel Figure 4a shows sectors of the Bloch sphere that can be reached by one motion and Figure 4b by two motions of the electron around the ring at various numbers of changes of the Rashba coupling during the revolution.

4 Effects of coloured noise on qubit transformations

For qubit transformations performed in linear systems, discussed in Section 2, the angle of spin rotation is proportional to the area in parametric space $[\xi, a_c]$ that is enclosed by the contour $a_c[\xi]$. In real situations, noise in driving functions $\alpha(t)$ and $\xi(t)$ will unavoidably arise due to electrostatic noise in gate potentials. Therefore, it is important to analyse the stability of the qubit transformation with respect to small deviations of drivings. The change in the angle of rotation is characterised by the change of the contour $a_c[\xi]$. Analogue effects are present also in ring systems discussed in Section 3. Here we show how to calculate and characterise the noise in $a_c(t)$, while the corresponding results for the position x (or φ in the case of ring

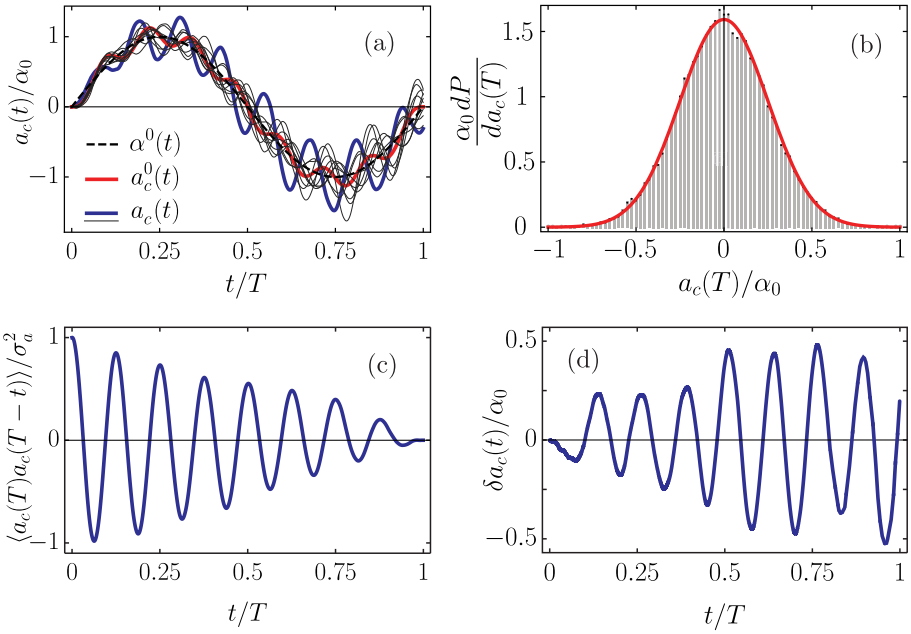

Fig. 5. All figures correspond to spin-orbit response $a_c(t)/\alpha_0$ to a sinusoidal driving with $n = 8$ and with a Gaussian white noise ($\tau_\alpha \to 0$) with noise intensity $\sigma_\alpha/\alpha_0 = \frac{1}{20}\omega^{-1/2}$. In (a) the dashed line marks the driving function without noise, the red one response to driving without noise and thin black lines the different realisations of response to noisy driving, one of which is marked with blue. In (b) the probability distribution of the final error in $a_c(T)/\alpha_0$ is shown with red curve corresponding to analytical result and black lines to numerical one. In (c) the autocorrelation function of $a_c(t)$ is shown and in (d) one realisation of noise in $a_c(t)$ (note the amplitude progressively increasing with time).

systems) can easily be derived in the same manner. Once this is analysed, one can analytically predict the angle of spin rotation error since analytic results for qubit transformations are known.

We model the noise as an additive coloured noise, $\alpha(t) = \alpha^0(t) + \delta\alpha(t)$, $\alpha^0(t)$ being the noiseless driving function and $\delta\alpha(t)$ the superimposed noise with vanishing mean $\langle\delta\alpha(t)\rangle$ and with the time autocorrelation function $\langle\delta\alpha(t')\delta\alpha(t'')\rangle = \frac{\sigma_\alpha^2}{2\tau_\alpha} e^{|t'-t''|/\tau_\alpha}$ characteristic for Ornstein-Uhlenbeck processes [39–42]. σ_α^2 is the noise intensity and τ_α the correlation time. As a general solution of equation (6) $a_c(t)$ is given by

$$a_c(t) = \omega \int_0^t \sin[\omega(t-t')]\alpha(t')\mathrm{d}t'. \tag{25}$$

In Figure 5 an explicit example of noise in $a_c(t)$ is shown. The driving is of sinusoidal form

$$\alpha^0(t) = \alpha_0 \cos(2\pi t/T_n), \tag{26}$$

with transformation times $T = T_n = nT_1$, where $T_1 = 2\pi/\omega$ is the period of the confining potential and $n > 1$. Driving in figures is for $n = 8$. The noise added is a short correlation one ($\tau_\alpha \to 0$) which corresponds to Gaussian white noise with σ_α.

Numerical calculation of $a_c(t)$ was done by summing over discrete values,

$$a_c(t) = a_c^0(t) + \sum_{i=1}^{N} \alpha_i a_i, \tag{27}$$

where $a_i = \omega \sin[\omega(t - t_i)]$, $t_i = i\Delta t$, $\Delta t = T/(N-1)$ and α_i is equal to the integral of the noise in a short time interval $\alpha_i = \int_{t_i}^{t_i+\Delta t} \delta\alpha(t')\,\mathrm{d}t'$. It is a stohastic normally distributed value with zero mean and with variance $\sigma_\alpha^2 \Delta t$ [44]. Figure 5a shows the driving noiseless function $\alpha^0(t)$ marked with black dashed line and red curve corresponds to $a_c^0(t)$ spin-orbit response to this noiseless driving. Blue line represents the response $a_c(t)$ to one realisation of noisy driving $\alpha(t)$. Some other responses to different noise realisations are marked with thin black lines. Final deviations of $a_c(T)$ from noiseless $a_c^0(T)$ are shown in Figure 5b as a normalised histogram (black bins) calculated from 10^7 noise realisations. Red curve corresponds to analytic result of the probability density function as is calculated in the following. As seen from the histogram, the response $a_c(T)$, an integral of stochastic variables, is normally distributed stochastic quantity in accordance with the central limit theorem. However, by looking at the nontrivial autocorrelation function $\langle a_c(T)a_c(T-t)\rangle$ in Figure 5c which oscillates with diminishing amplitude, the variance of distribution σ_a^2 seems to be nontrivial in time-dependence. This can be further speculated from Figure 5d which shows bare noise in spin-orbit response $\delta a_c(t)$ as a function of time and it is evident that it oscillates with confining potential frequency and grows in amplitude. We evaluate σ_a^2 as equal-times autocorrelation function [40,43],

$$\sigma_a^2(t) = \omega^2 \lim_{\Delta t \to 0} \Big\langle \int_0^t \sin[\omega(t-t')]\delta\alpha(t')\mathrm{d}t' \int_0^{t+\Delta t} \sin[\omega(t-t'')]\delta\alpha(t'')\mathrm{d}t'' \Big\rangle. \tag{28}$$

This is calculated as an integral after leaving in average $\langle\rangle$ the only stochastic term $\delta\alpha(t')\delta\alpha(t'')$ and evaluating it as the time autocorrelation function. For the Ornstein-Uhlenbeck noise considered here the integrals can be evaluated analytically and the final result is that $a_c(t)$ is distributed normally with the time dependent variance

$$\begin{aligned}\sigma_a^2(t) = \frac{\omega\sigma_\alpha^2}{4(1+\omega^2\tau_\alpha^2)^2}\big[&-4\omega^2\tau_\alpha^2 e^{-t/\tau_\alpha}(\omega\tau_\alpha\cos\omega t + \sin\omega t) \\ &+ 2\omega t - \omega\tau_\alpha + \omega^3\tau_\alpha^2(2t+3\tau_\alpha) + (1+\omega^2\tau_\alpha^2)(\omega\tau_\alpha\cos 2\omega t - \sin 2\omega t)\big].\end{aligned} \tag{29}$$

In short correlation time limit the expression simplifies to the white noise result, $\sigma_a^2(t) = \frac{1}{4}\omega\sigma_\alpha^2\,(2\omega t - \sin 2\omega t)$. For large ωt the noise amplitude diverges and the reason is that the Lorentzian noise power spectrum $\sigma_\alpha^2/[1 + (2\pi f\tau_\alpha)^2]$ considered here consists of different driving frequencies including the resonant value $\omega = 2\pi f$ which, similar to the one-dimensional random walk problem [40], results in the asymptotic response $\sigma_a^2(t) \propto t$. This indicates that fast transformations are preferable since less noise is produced. Qualitatively the same arguments are valid also for qubit transformations on ring systems considered in Section 3.

5 Summary

Holonomic spin manipulation in linear systems is feasible if one can control the position $\xi(t)$ of the electron confining potential and the strength of the Rashba coupling $\alpha(t)$. In the space of these two driving parameters $[\xi, \alpha]$ an arbitrary contour

determines the angle of the qubit rotation in the case of adiabatic transformation. For a broad range of integrable drivings exact solutions are possible and a natural question arises: Which one of the non-adiabatic and adiabatic transformations leads to larger or smaller qubit rotation? In this paper we demonstrated that the answer crucially depends on the contour in spaces $[\xi, \alpha]$ and $[\xi, a_c]$. In particular, we showed that compared to the adiabatic result some non-adiabatic transformation angles can be larger, while for other transformations smaller. Both angles can also be equal for some contours. There seems to be no general rule.

The main drawback of qubit transformations in linear systems is the restriction to transformations represented by rotations around a fixed axis. This limitation is lifted if the electron can be moved on a ring system. Exact solutions of qubit dynamics are available, however, the corresponding equations do not allow to analytically determine driving parameters for arbitrary final qubit state. This was the motivation to analyse various driving schemes numerically and we demonstrated that an arbitrary final state on the Bloch sphere is reachable providing corresponding drivings.

To conclude, we examined in detail also the influence on qubit transformations due to the noise in drivings. Since analytical treatment of several driving schemes is possible one can analyse also the effects of noise exactly. We demonstrated how the errors in driving give rise to variance in the spin-orbit response function. It is shown how one can analyse the effects of a general coloured noise and as an example, we show the result for the Ornstein-Uhlenbeck noise, also in the limit of short correlation times (white noise). Analytical results for autocorrelation function and time dependent errors are tested numerically.

A.R. and L.U. acknowledge partial support from the Slovenian Research Agency under contract no. P1-0044 and T.Č. the support by the National Natural Science Foundation of China (NSFC) Grant No. 11650110443.

References

1. S.A. Wolf, D.D. Awschalom, R.A. Buhrman, J.M. Daughton, S. von Molnár, S.M. Roukes, A.Y. Chtchelkanova, D.M. Treger, Science **294**, 1488 (2001)
2. R. Hanson, L.P. Kouwenhoven, J.R. Petta, A. Tarucha, L.M.K. Vandersypen, Rev. Mod. Phys. **79**, 1217 (2007)
3. F.H.L. Koopens, C. Buizert, K.J. Tielrooij, I.T. Vink, K.C. Nowack, T. Meunier, L.P. Kouwenhoven, L.M.K. Vandersypen, Nature **442**, 766 (2006)
4. G. Dresselhaus, Phys. Rev. **100**, 580 (1955)
5. Y.A. Bychkov, E.I. Rashba, J. Phys. C: Solid State Phys. **17**, 6039 (1984)
6. D. Stepanenko, N.E. Bonesteel, Phys. Rev. Lett. **93**, 140501 (2004)
7. C. Flindt, A.S. Sørensen, K. Flensberg, Phys. Rev. Lett. **97**, 240501 (2006
8. W.A. Coish, V.N. Golovach, J.C. Egues, D. Loss, Phys. Status Solidi (b) **243**, 3658 (2006)
9. P. San-Jose, B. Scharfenberger, G. Schön, A. Shnirman, G. Zarand, Phys. Rev. B **77**, 045305 (2008)
10. V.N. Golovach, M. Borhani, D. Loss, Phys. Rev. A **81**, 022315 (2010)
11. S. Bednarek, B. Szafran, Phys. Rev. Lett. **101**, 216805 (2008)
12. F. Jingtao, C. Yuansen, C. Gang, X. Liantuan, J. Suotang, N. Franco, Sci. Rep. **6**, 38851 (2016)
13. A. Gómez-León, G. Platero, Phys. Rev. B **86**, 115318 (2012)
14. J. Pawlowski, P. Szumniak, S. Bednarek, Phys. Rev. B **93**, 045309 (2016)
15. J. Pawlowski, P. Szumniak, S. Bednarek, Phys. Rev. B **94**, 155407 (2016)
16. S. Nadj-Perge, V.S. Pribiag, J.W.G. van den Berg, K. Zuo, S.R. Plissard, E.P.A.M. Bakkers, S.M. Frolov, L.P. Kouwenhoven, Phys. Rev. Lett. **108**, 166801 (2012)

17. S. Nadj-Perge, S.M. Frolov, E.P.A.M. Bakkers, L.P. Kouwenhovenx, Nature **468**, 1084 (2005)
18. C. Fasth, A. Fuhrer, M.T. Björk, L. Samuelson, Nano Lett. **5**, 1487 (2005)
19. C. Fasth, A. Fuhrer, L. Samuelson, V.N. Golovach, D. Loss, Phys. Rev. Lett. **98**, 266801 (2007)
20. S.K. Shin, S. Huang, N. Fukata, K. Ishibashi, Appl. Phys. Lett. **100**, 073103 (2012)
21. T. Čadež, J.H. Jefferson, A. Ramšak, New J. Phys. **15**, 013029 (2013)
22. T. Čadež, J.H. Jefferson, A. Ramšak, Phys. Rev. Lett. **112**, 150402 (2014)
23. J. Nitta, T. Akazaki, H. Takayanagi, T. Enoki, Phys. Rev. Lett. **78**, 1335 (1997)
24. D. Liang, X.P.A. Gao, Nano Lett. **12**, 3263 (2012)
25. J. Anandan, Phys. Lett. A **133**, 171 (1988)
26. A. Kregar, J.H. Jefferson, A. Ramšak, Phys. Rev. B **93**, 075432 (2016)
27. A. Kregar, A. Ramšak, Int. J. Mod. Phys. B **30**, 1642016 (2016)
28. L. Ulčakar, A. Ramšak, New J. Phys. **19**, 093015 (2017)
29. P. San-Jose, G. Zarand, A. Shnirman, G. Schön, Phys. Rev. Lett. **97**, 076803 (2006)
30. P. Huang, X. Hu, Phys. Rev. B **88**, 075301 (2013)
31. C. Echeverría-Arrondo, E.Y. Sherman, Phys. Rev. B **87**, 081410(R) (2013)
32. J. Mravlje, A. Ramšak, T. Rejec, Phys. Rev. B **74**, 205320 (2006)
33. J. Mravlje, A. Ramšak, Phys. Rev. B **78**, 235416 (2008)
34. G. Giavaras, J.H. Jefferson, A. Ramšak, T.P. Spiller, C. Lambert, Phys. Rev. B **74**, 195341 (2006)
35. T. Rejec, A. Ramšak, J.H. Jefferson, J. Phys.: Condens. Matter **12**, L233 (2000)
36. J.H. Jefferson, A. Ramšak, T. Rejec, Europhys. Lett. **74**, 764 (2006)
37. F. Wilczek, A. Zee, Phys. Rev. Lett. **52**, 2111 (1984)
38. F.E. Meijer, A.F. Morpurgo, T.M. Klapwijk, Phys. Rev. B **66**, 033107 (2002)
39. G.E. Uhlenbeck, L.S. Ornstein, Phys. Rev. **36**, 823 (1930)
40. M.C. Wang, G.E. Uhlenbeck, Rev. Mod. Phys. **17**, 323 (1945)
41. J. Masoliver, Phys. Rev. A **45**, 706 (1992)
42. J. Heinrichs, Phys. Rev. E **47**, 3007 (1993)
43. W. Feller, in *An Introduction to Probability Theory and its Applications* (Wiley, New York, 1971), Vol. 1, p. 2
44. I.M. Sokolov, W. Ebelling, B. Dybiec, Phys. Rev. E **83**, 041118 (2011)